Fluorescent-Core Microcavities based on Silicon Quantum Dots for Oil Sensing Applications

V. Zamora, Z. Zhang, and A. Meldrum

Abstract—The compatibility of optical resonators with microfluidic systems may be relevant for chemical and biological applications. Here, a fluorescent-core microcavity (FCM) is investigated as a refractometric sensor for heavy oils. A high-index film of silicon quantum dots (QDs) was formed inside the capillary, supporting cylindrical fluorescence whispering gallery modes (WGMs). A set of standard refractive index oils was injected into a capillary, causing a shift of the WGM resonances toward longer wavelengths. A maximum sensitivity of 240 nm/RIU (refractive index unit) was found for a nominal oil index of 1.74. As well, a sensitivity of 22 nm/RIU was obtained for a lower index of 1.48, more typical of fuel hydrocarbons. Furthermore, the observed spectra and sensitivities were compared to theoretical predictions and reproduced via FDTD simulations, showing in general an excellent agreement. This work demonstrates the potential use of FCMs for oil sensing applications and the more generally for detecting liquid solutions with a high refractive index or high viscosity.

Keywords—Oils,optical resonators, sensing applications,whispering gallery modes.

I. INTRODUCTION

MICROCAPILLARIES are currently receiving a significant degree of attention because of their properties as optical resonators, which can be important for bio- and chemical sensing applications. Liquid-core optical ring resonators (LCORRs) are thin-walled capillaries that offer a high sensitivity response, label-free detection and compatibility with microfluidic systems, among other important features[1]. Because of the thin capillary walls, a fraction of the electric field of whispering gallery modes (WGMs) extends into the channel of the capillary, while a part of it spreads into the space outside, as required for external coupling. Thus, the WGMs can be measured via evanescent coupling from a single-mode fiber interfaced to a tuneable laser, while a change in refractive index of the medium in the channel causes a wavelength shift of the resonance. This optical detection method can be exploited for bulk sensing applications, for example, to determinate the concentrations of ethanol [1] and glucose diluted in water [2], flowing through the capillary channel. For biomolecule recognition applications, the specific binding of target biomolecules at the chemically functionalized surface of LCORRs gives a local change in refractive index, resulting in a change in resonance wavelength. A variety of biomolecules such as viruses [3], proteins [4], DNA [5] and pesticides [6], [7] have been detected using LCORRs. However, LCORRs have not been investigated as optical sensors in the petro- and chemical industry field. In general, the microfluidic system development for oil- and gas sensing applications has seen only a few investigations [8], [9].

The sensitivity of such optical devices depends on the structural parameters. To achieve an interaction with the analyte in channelrequires a reduction in the LCRRs wall thickness to the micrometer scale (or submicrometer) via chemical process [1] or a combination of inflation and tapering [2].Thus, LCORRs are difficult to fabricate and are mechanically fragile. In addition, the characterization method is expensive and fairly difficult in practice, because it requires a tunable laser and nanopositioning equipment to measure the resonance.

Recently, we proposed analternative device for refractometric detection of water-based solutions [10]. This device is similar to an LCORR, in that it relies on the cylindrical WGMs of a capillary for detection. However, the main structural difference is that the fluorescent-core microcavity (FCM)consists of a film of fluorescent silicon quantum dots (QDs), about 500 nm thick, adhered to the inner surface of the microcapillary (Fig. 1). The film has a high refractive index about 1.67 [10], and thus can support WGM resonances mainly confined within the film itself, due to the lower refractive index of the capillary wall (n_{silica}=1.452). This FCM does not require evanescent coupling, since the WGMs appear as maxima in the emitted fluorescence spectra. This device presents a robust, durable and reusable optical sensor that requires neither a thinning treatments nor evanescent coupling. However, as discussed below, these advantages come with a trade-off with respect to the minimum detection limits.

The object of the present work was to demonstrate the refractometric response of FCMs to high-index oils. The oils are more viscous than water solutions, suggesting a potential difficulty for injection into the FCMs.We utilized calibrated refractive index oils, with indices varying from 1.46 to 1.75, which spans (and exceeds) the highest-index range reported for most commercial hydrocarbon products [11], [12].At the same time, this experiment aimed to understand the behavior of the fluorescence WGMs when the refractive index of the channel is higher than that of the QD film.

V. Zamora was with the Department of Physics, University of Alberta, Edmonton, AB T6G2E1 CA. She is now with the Department of High Speed Hardware Architectures, HHI-Fraunhofer Institute, Berlin, 10587 DE (phone: +4930-31002-338; e-mail: vanessa.zamora@hhi.fraunhofer.de).

Z. Zhang is with the Department of Physics, University of Alberta, Edmonton, AB T6G2E1 CA (e-mail: zhihong@ ualberta.ca).

A. Meldrum is with the Department of Physics, University of Alberta, Edmonton, ABT6G2E1CA (e-mail: ameldrum@ ualberta.ca).
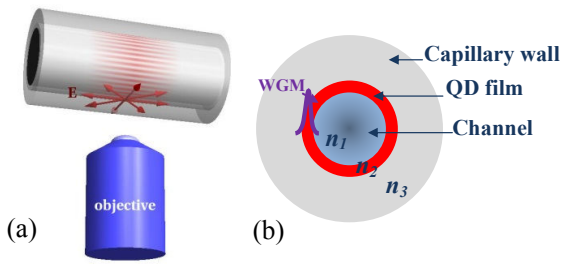
Fig. 1 (a) Schematic of the device structure, illustrating the development of the WGM resonances confined into the film. The scattered fluorescence is collected with a microscope objective. (b) Schematic cross section of the FCM, illustrating the WGM field intensity (purple "wave"). Here the tail of the field interacts with the analyte medium in the channel

II. THEORETICAL ANALYSIS

The WGM resonances were calculated using the perturbation theory developed by Teraoka and Arnold [13], modified to account for the cylindrical symmetry of the capillary. This allows the identification of each of the experimental peak and a calculation of refractometric sensitivity to be performed. The modeling is based on Maxwell′s equations for the electrical field of a 3-layer cylinder. In order to satisfy Maxwell's equations, the solutions for the electric field in each medium are given by

$$E_{n,l}(r) = \begin{cases} A_l J_l(n_1 kr) & r < a-t \\ B_l J_l(n_2 kr) + C_l Y_l(n_2 kr) & a-t < r < a \\ D_l Y_l(n_3 kr) & r > a \end{cases} \quad (1)$$

where n and l are the radial and angular order of the resonance, respectively. The refractive indices n_1, n_2 and n_3 correspond to the channel, QD film and capillary wall, a is the capillary inner radius, and t is the film thickness. The capillary outer diameter extends to infinity. J_l and Y_l are the cylindrical Bessel functions of the first and second kind, which describe the radial behavior of the electric field for each region. The boundary conditions are imposed at the interface, which for the TE polarization implies that the fields and their derivatives are continuous. With these boundary conditions, the solutions to (1) permit the field distribution and sensitivity to be directly estimated [14].

To illustrate the evolution of the electric field intensity distribution and refractometric sensitivity as a function of the channel index n_1, four examples are presented in Fig.2. The electric field distribution of the resonance is confined completely into the QD film. When the refractive index of the channel increases from 1.0 to 1.7, the field of the fundamental mode is gradually *pulled* inside the channel. One example of second-order radial modes is included for n_1=1.7 (Fig. 2c). Once more, the field shows the similar effect. For n_1=1.7, a significant part of the field extends into the channel.
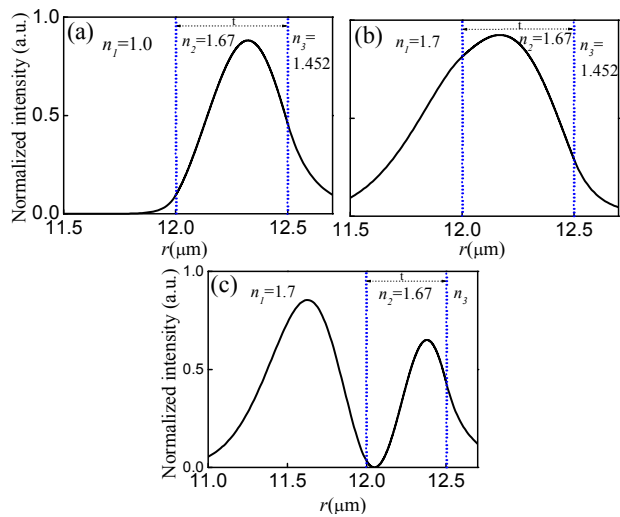

Fig. 2 Electric field intensity profile for the fundamental mode, n=1 and l=155, when the channel is filled with: (a) air (n_1=1.0) and (b) a refractive index oil of n_1=1.7. The second radial order mode (n=2 and l=155) is included for (c) n_1=1.7. The dashed lines show the interfaces of the three mediums. Parameters: a=12.5 μm, t=500 nm, n_2=1.67 and n_3=1.452

For lower refractive indices, theoretical sensitivitiesare lower, for example, we calculate a sensitivity of 11.2 nm/RIU (refractive index unit) for the first-radial order mode, when the channel index is 1.33. For a high refractive index of 1.75, the sensitivity is 309nm/RIU, which increases as a function of n_1. The sensitivity corresponding to the second-radial order mode is 270 nm/RIU for the same index of1.75, which is slightly lower than the fundamental mode.

III. FABRICATION AND CHARACTERIZATION METHODS

The FCM fabrication method has been described in detail in previous work [15]. Commercially available silica microcapillaries (Polymicro Technologies) with a nominal inner and outer diameter of 25 μm and 360 μm, respectively, were used in these experiments. Briefly, the polyimide jackets were removed by ashing, and the capillaries werethen dipped into asolution of hydrogen silsesquioxane (HSQ) dissolved in methyl isobutyl ketone (MIBK). During the dipping procedure, the solution flows upward into the channeldue to capillary forces. After filling, the capillaries were annealed in a 95%Ar + 5% H_2 forming gas mixture, in a two-stage process. Stage 1 was at 300 °C for three hours, and Stage 2 was at 1100 °C for one hour. The samples were then slow-cooled to room temperature over a 12-hour period. Using this method, asilicon QD film with a thickness near half a micrometer and a refractive index near 1.67 can be formed on the channel surface [10].

The cylindrical optical resonances were excited by pumping the QDs with the 488-nm line of an Argon-ion laser (Coherent Innova 70C Spectrum). Typically, the incident laser beam had apump power on the sample about 45mW. The beam is incident through free space onto side of the capillary, and the emitted fluorescence is collected by the objective lensof a fluorescence microscope (Nikon TE-2000E). An analyzer was

used in the light path in order to collect either the TE or TM polarized WGMs. A spectrometer (the SGS unit from the Santa Barbara Instruments Group) with a nominal resolution of 0.24 nm and a CDD pitch of 0.1 nm/pixelwasutilized to measure the fluorescence spectrum. The spectra were calibrated for wavelength and intensity by using a HgAr lamp and a blackbody radiator (the LS1 light source from Ocean Optics).

The microfluidic set up consisted of a micropump connected to one end of the capillary via a syringe and a length of polyethylene tubing. The oil sets are sold by Cargille Laboratories [16] and cover a refractive index range from 1.46 to 1.75. These nominal values are for a temperature of 25°C and a wavelength of 589 nm. In the rest of the paper, we will refer to the oils by citing these nominal values, but dispersion was taken into account when necessary (*e.g.*, for simulations) by using the Cauchy relations provided by the manufacturer. For each measurement, the channel was cleaned by pumping clean methanol for 15 minutes, followed by the injection of each oil to be analyzed.

IV. RESULTS AND DISCUSSION

The QD film in the capillary appeared smooth and featureless. In the transmission images, the film appeared as an amber tint that was confined to the capillary channel (Fig. 3a). The fluorescence image (Fig. 3b) also appeared uniform, with a particularly bright region located near the channel walls. We find that these features are characteristic of good samples that show well-developed WGMs.
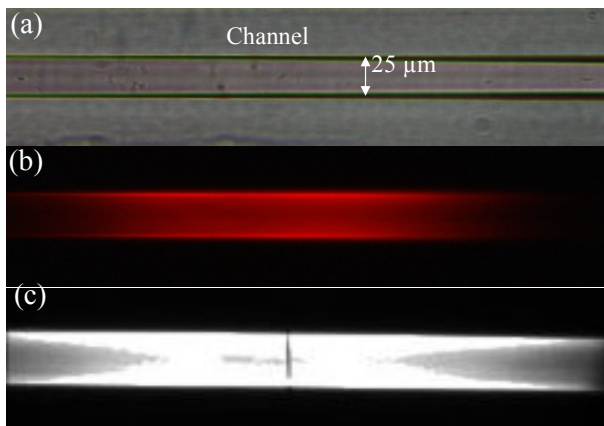

Fig. 3 (a) Transmitted light image of a capillary whose channel surface is coated with a QD film about 500 nm thick. The capillary channel is empty (n_1=1.0). (b) Fluorescence image of the same capillary. The position of the slit near center of the monochrome "tracking image"in (c) corresponds to the spectral image in Fig.4a. Capillary parameters: inner and outer diameter of 25 μm and 360 μm

WGM resonances appeared as well-defined oscillations in the fluorescence spectrum. To obtain the emission spectra, spectrum images were taken with the slit perpendicular to the capillary axis (see Fig. 3c) and the analyzer transmission axis parallel to the capillary channel (i.e., TE polarization). One such spectrum image is shown in Fig. 4a. A set of intensity

oscillations is clearly visible in regions corresponding to the bright channel walls in Fig. 3b and 3c. In order to obtain a conventional 1D spectrum, a region of the spectral image was cropped, summed vertically, and plotted in Fig. 4b. Each peak in the spectrum corresponds to the excitation of a WGM resonance. These resonances can be characterized by a quality factor ($Q = \lambda_{peak}/\Delta\lambda_{peak}$) around of 500 and free spectral range (FSR) about 4.5nm (Fig. 4b).The short-wavelength skewing of the WGMs is probably caused by the simultaneous excitation of spiraling modes; *i.e.*, WGMs having a small component of the wavevector in the z-direction [10], [17].
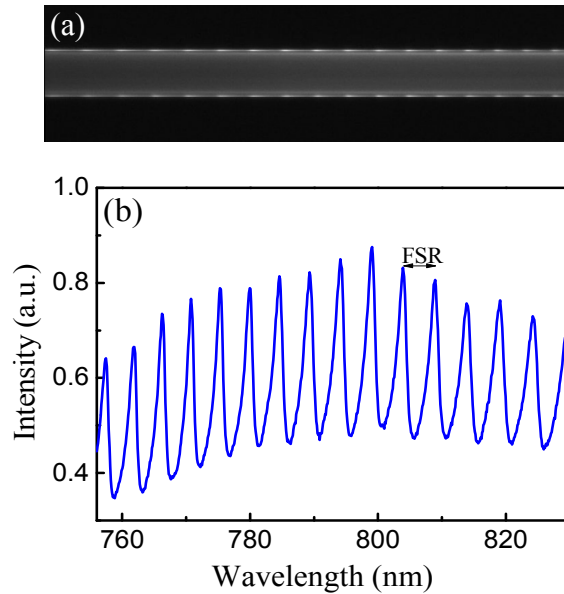

Fig. 4 WGM resonances observed in the FCM for n_1=1.0 (i.e., air in the channel). (a) Spectral image (b) spectrum cropped from (a) showing sharp WGMs having to the transverse electric (TE) polarization

The WGMs in the fluorescence spectra evolved in several ways, as the channel refractive index fluid increased from 1.46 to 1.75 (Fig. 5a). Here, a spectrum for methanol (1.32) is included; it was used as a reference to ensure that the capillary was clean prior to each subsequent measurement. In Fig. 5b, the resonances centered at 789.95 nm and 798.97 nm, for a channel index of 1.32, were followed as the refractive index of the channel fluid increased to 1.75. First the TE-polarized WGMs shifted to longer wavelengths as a function of theoil index n_1. As n_1 approached the film index (blue dashed line in Fig. 5b), a second family of resonances appeared in the spectra (this is highlighted by the pink square in Fig. 5b, within which both mode families were present). Finally, at the highest oil refractive index, only a single family of WGMs was again present in the spectrum. In Fig. 5b the dispersion of the oils was used to obtain the appropriate x-axis coordinate in the two experimental curves, using the Cauchy constants provided by the manufacturer. The calibrated oil index was chosen in fluorescence emission range.

To understand the WGM spectra of the oils, they were modeled with 2D finite-difference- time-domain (FDTD) simulations. Initially, the parameters of the theoretical model were used as input for the simulations. Next, the index and thickness of film were slightly adjusted until the FDTD solutions closely reproduced the experimental spectrum for channel indices of 1.46 and 1.75. Dispersion for the silica capillary wall and the refractive index oil was taken into account, but the QD layer was assumed to have a fixed refractive index. The grid size, matching layers, and number of time steps were chosen by following the standard procedures described in [18].
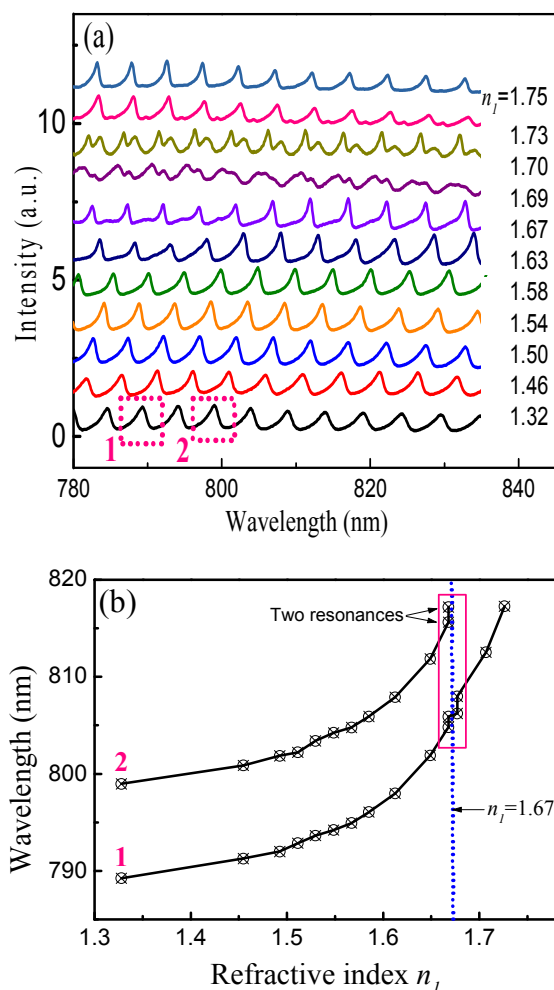

Fig. 5 (a) Evolution of the fluorescence spectrum, starting from methanol (n_1=1.32), and subsequently pumpingoils into the channel with nominal refractive indices ranging from 1.46 to 1.75. The spectral shift of two peaks centered at λ = 789.95 nm and 798.97 nm, respectively, for n_1 = 1.32 re traced out in (b). The dashed line marks the refractive index value of the QD film. The square encompasses the range of refractive indices for which two families of modes were observed. The lines connecting the points are a guide to the eye

The FDTD simulations and the experimental spectra show a good agreement for a film thickness of 475 nm, a film index of

1.675 and capillary inner diameter of 25 μm. This agreement is evident in Fig. 6, where three spectra with different channel refractive indices have been compared. In the first case, the channel index is lower than the index of the film, $n_1 < n_2$ (Fig. 6a). Here the spectrum presents a family of peaks that belongs to the first-order radial modes (n=1). In the second case, the channel index is nearly equal to the film index, i.e. $n_1 \approx n_2$ (Fig. 6b). The initial family of maxima has become weaker, while new family of modes appears in the spectrum. From the FDTD simulations, this new set of maxima corresponds to the second-radial order modes (n=2). The spectrometer resolution can cause the two closely-separated peaks to appear overlapped, but the agreement between the experimental and simulated spectra in Fig 6b is nevertheless quite clear. When the channel index becomes greater than the film index, $n_1 < n_2$, the second-order radial peaks become stronger than the first-order radial ones. At the highest oil refractive index, the spectrum is essentially composed only of second-order radial order modes. As a complementary example, Fig 6d shows the identified WGM resonance from Fig. 5b.

A parameter of interest for sensing applications is the sensitivity, defined as the wavelength shift per change in refractive index, $\delta\lambda/\delta n_1$. For a low channel index of 1.48, the experimental sensitivity is 22.5 nm/RIU and the theoretical sensitivity is 22.9 nm/RIU for the parameters used in the simulations. For a high channel refractive index of 1.74, the experimental sensitivity is 240 nm/RIU; whereas the theoretical sensitivity is 265 nm/RIU for the second-order radial mode (*i.e.*, the modes that dominate the spectrum for these high indices). As a preliminary conclusion, 240 nm/RIU is to our knowledge the highest refractometric sensitivity reported for fluorescence WGMs, being comparable in magnitude to some of the highest values obtained with resonators that useevanescent field coupling [1], [2]. Based on a sensitivity of 240 nm/RIU and a detection limit of 10 pm for fluorescence WGMs [19], the optimal resolution limit is on the order of 4 x 10^{-5} RIU.

During the last two decades, the microfluidic technology has been developed and successfully employed for analyzing a variety of target biomolecules [20]-[22]. In contrast, hydrocarbon analysis in real-time and in small amounts (microliter scale) has yet to be widely investigated in the petrochemical industry. Due to the growing demand to reduce the costs and analysis time [23]-[25] (*e.g.*, using mass spectroscopy), durable, microfluidic-compatible optical resonators could present a possible alternative for viscous hydrocarbon analysis. Obviously, just as with biosensors, if specificity is required it will be necessary to treat the channel surface for the binding of specific target molecules. This could represent a particularly interesting challenge, since commercial hydrocarbons are typically composed of varying concentrations of numerous separate components and impurities. Finally, a practical portability and low-cost could be enabled, by using a light emitting diode (LED) source and integrated microspectrometer for detecting a specific analytes in real conditions.
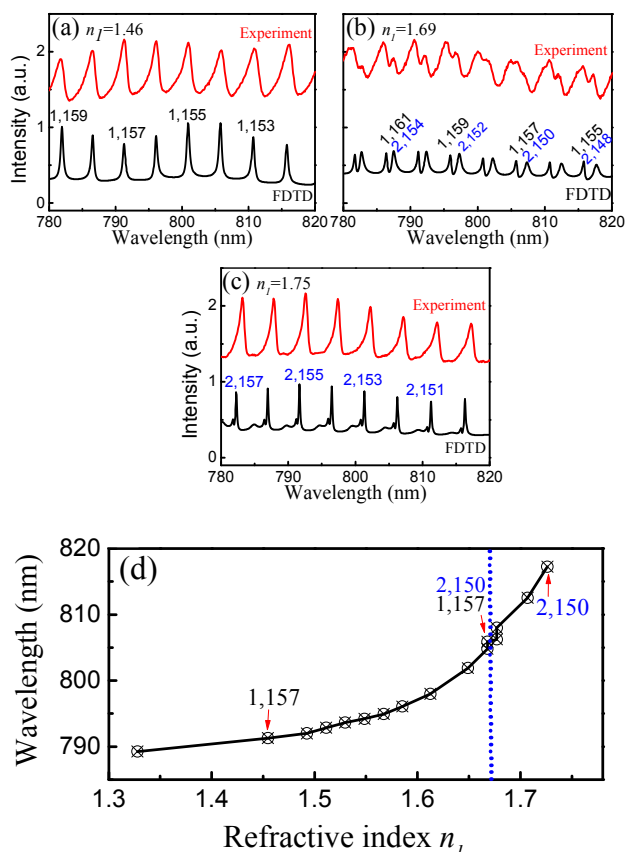
Fig. 6 Comparison of FDTD simulations (black spectra) with experiment (red spectra) for three different nominal oil indices: (a) 1.46, (b) 1.69 and (c) 1.75. The peaks are labeled with their radial, n, and angular, l, order numbers. (d) Example of the identified resonance centered at 789.95 nm. Simulation parameters: t=475 nm, n_2=1.675 and n_3= 1.452

V. CONCLUSION

An optical device based on a fluorescent-core microcavityfor heavy oil detection was reported. The fluorescence WGM characterization of calibrated oils was carried out successfully, using a microcapillary with a layer of silicon quantum dots coated on the channel surface. The WGMs show a high sensitivity for oils, especially those with a refractive index higher than that of the QD film. The spectrum evolves uniformly from one dominated by first-order radial modes to one composed entirely of second-radial modes as the refractive index of the oil in the capillary channel increased from nominally 1.46 to 1.75. Overall good agreement was obtained between the experimental results and FDTD simulations. A maximum sensitivity of 240 nm/RIU was found for an oil index of 1.74. This value is the highest reported for fluorescence microresonators and agrees well with the theoretical estimation. The detection limit was estimated in the range of 10^{-4} to 10^{-5} RIU for FCMs, which is highly competitive with other fluorescence WGM-based sensors.

REFERENCES

[1] I.M. White, H. Oveys and X. Fan, "Liquid-core optical ring-resonator sensors," *Opt. Lett.*, vol. 31, no. 9, pp. 1319-1321, May 2006.
[2] V. Zamora, A. Diez, M.V Andres and B. Gimeno, "Cylindrical optical microcavities: basic properties and sensor applications," *Photonics and Nanostructures – Fundamentals and Applications*, vol. 9, no. 2, pp. 149-158, Sept. 2011.
[3] H. Zhu, I. M. White, J. D. Suter, M. Zourob and X. Fan, "Opto-fluidic micro-ring resonator for sensitive label-free viral detection," *Analyst*, vol. 133, no. 3, pp. 356-360, Jan. 2008.
[4] H. Zhu, I. M. White, J. D. Suter and X. Fan, "Phage-based label-free biomolecule detection in an opto-fluidic ring resonator," *Biosens. Bioelectron.*, vol. 24, no. 3, pp. 461-466, Nov. 2008.
[5] J.D. Suter, I.M. White, H. Zhua, H. Shi, C.W. Caldwell and X. Fan, "Label-free quantitative DNA detection using the liquid core optical ring resonator," *Biosens. Bioelectron.*, vol. 23, no. 7, pp. 1003-1009, Feb. 2008.
[6] G. Yang, I.M. White, and X. Fan, "An opto-fluidic ring resonator biosensor for the detection of organophosphorus pesticides," *Sens. Act. B: Chemical*, vol. 133, no.1, pp. 105-112, Jul. 2008.
[7] S. Lee, J-H Moon and G. Kim, "Detection of 6-benzylaminopurine plant bioregulator using an opto-fluidic ring resonator (OFRR) biosensor," *Anal. Methods*, vol. 4, no. 4, pp. 1041-1045, Mar. 2012.
[8] D.E. Angelescu, B. Mercier, D. Siess and R. Schroeder, "Microfluidic capillary separation and real-time spectroscopic analysis of specific components from multiphase mixtures," *Anal. Chem.*, vol. 82, no. 6, pp. 2412-2420, Feb. 2010.
[9] M-J. Tsang, M. Ching, A.E. Pomerantz, A.B. Andrews, P. Dryden, R. Schroeder, O.C. Mullins and C. Harrison, "On the nanofiltration of asphaltene solutions, crude oils, and emulsions," *Energy Fuels*, vol. 24, no.9, pp. 5028-5037, Aug. 2010.
[10] C. P. K. Manchee, V. Zamora, J. W. Silverstone, J. G. C. Veinot and A. Meldrum "Refractometric sensing with fluorescent-core microcapillaries," *Opt. Express*, vol. 19, no.22 , pp. 21540-21551, Jan. 2011.
[11] J. Castillo, H. Gutierrez, M. Ranaudo and O. Villarroel, "Measurement of the refractive index of crude oil and asphaltene solutions: onset flocculation determination," *Energy Fuels*, vol. 24, no.1, pp. 492-495, Nov. 2010.
[12] H. El Ghandoor, E. Hegazi, I. Nasser and G.M. Behery, "Measuring the refractive index of crude oil using a capillary tube interferometer," *Opt. Laser Tech.*, vol. 35, pp. 361-367, Jan. 2003.
[13] I. Teraoka and S. Arnold, "Enhancing the sensitivity of a whispering-gallery mode microsphere sensor by a high-refractive-index surface layer," *JOSA B*, vol. 23, no. 7, pp. 1434-1441, Jul. 2006.
[14] I. Teraoka, S. Arnold and F. Vollmer, "Perturbation approach to shift of whispering-gallery-modes in microspheres by protein adsorption," *JOSA B*, vol. 20, no. 9, pp.1937-1946, Sept. 2003.
[15] J. R. Rodriguez, P. Bianucci, A. Meldrum and J. G. C. Veinot, "Whispering gallery modes in hollow cylindrical microcavities containing silicon nanocrystals," *Appl. Phys. Lett.*, vol. 93, no. 13, pp. 131119, Mar. 2008.
[16] http://www.cargille.com/
[17] A.W. Poon, R.K. Chang and J.A. Lock, "Spiral morphology-dependent resonances in an optical fiber: effects of fiber tilt and focused gaussian beam illumination," *Opt. Lett.*, vol. 23, no.14, pp. 1105-1107, Jul. 1998.
[18] A. V. Boriskin, S.V. Boriskina, A. Rolland, R. Sauleau, and A. I. Nosich, "Test of the FDTD Accuracy in the Analysis of the Scattering Resonances Associated With High-Q Whispering-Gallery Modes of a Circular Cylinder, " *JOSA A*, vol. 25, no.5, pp. 1169-1173, May 2008.
[19] J. W. Silverstone, S McFarlane, C.P.K. Manchee and A Meldrum, "Ultimate Resolution for Refractometric Sensing With Whispering Gallery Mode Microcavities," *Opt. Express*, vol. 20, no. 9, pp. 8284-8295, Apr. 2012.
[20] D. J. Beede, G. A. Mensing and G. M. Walter, "Physics and applications of microfluidics in biology," *Annu. Rev. Biomed. Eng.*, vol. 4, pp. 261-286, Aug. 2002.
[21] J. Noh, H. C. Kim and D. Chung,"Biosensors in microfluidic chips," *Top. Curr. Chem.*, vol. 304, pp. 117-152, Apr. 2011.
[22] S. G. Fiorini and D. T. Chiu, "Disposable microfluidic devices: fabrication, function, and application," *BioTechniques*, vol. 38, pp. 429-446, Mar. 2005.
[23] P. R. Lewis, P. Maginell, D. R. Adkins, R. J. Kottenstette, D.R.Wheeler, S. S. Sokolowski, D.E. Trudell, J.E. Byrns, M. Okandan, Bauer J.M.,

R.G. Manley and C.Frye-Mason, "Recent advancements in the gas-phase microchemlab, " *IEEE Sensors Journal*, vol. 6, no. 3, pp. 784-795. Jun.2006.

[24] R. Camilli, "Characterizing marine hydrocarbons with in-situ mass spectrometry," in *Oceans 2007 IEEE Conf.*, pp. 1-7.

[25] R. Camilli, B. Bingham, C. M. Reddy, R. K. Nelson and A. N. Duryea, "Method for rapid localization of seafloor petroleum contamination using concurrent mass spectrometry and acoustic positioning," *Marine Pollution Bulletin*, vol. 58, no. 10, pp. 1505-1513, Jun.2009.

Vanessa Zamora was born in Ebano, Mexico, in 1981. She received her Ph.D. degree in Physics from University of Valencia, Spain, in 2010. Previously, she received her M.Sc.A. and B.Sc.degrees in Applied Physics and Physics Engineering from University of San Luis Potosi, Mexico. Dr. Zamora was a postdoctoral fellow at the department of Physics of the University of Alberta, Canada. Currently, she is a research associate at the Department of High Speed Hardware Architectures of the HHI-Fraunhofer Institute, Germany. Her current research interests are focused in the area of optical resonators for biosensing applications.